Dynamical effects at avoided level crossings: A study of the Landau-Zener effect using Rydberg atoms

Jan R. Rubbmark, Michael M. Kash, Michael G. Littman,* and Daniel Kleppner
Research Laboratory of Electronics and Department of Physics, Massachusetts Institute of Technology, Cambridge, Massachusetts 02139
(Received 16 January 1981)

We present a study of the dynamics of traversing an avoided energy level crossing. A pair of Stark levels of Rydberg states of lithium are used as a test system for measuring the diabatic transition probability. The experimental conditions are close to those assumed by the Landau-Zener theory. Possible corrections to the Landau-Zener theory are analyzed, and applications of the results to pulsed-field ionization are discussed.

I. INTRODUCTION

Nonadiabatic transitions at avoided crossings between potential curves have long been known to play a fundamental role in inelastic molecular collisions. The most elementary case—transitions at an avoided crossing of two levels which are traversed linearly in time—was analyzed in the early days of quantum mechanics by Landau[1] and Zener,[2] and is known as the Landau-Zener effect. Their calculation has served as the starting point for studies of phenomena such as energy exchange, charge exchange, and predissociation and associative recombination.[3] The Landau-Zener effect can also be important in atomic systems. For instance, adiabatic rapid passage of a two-level system is accurately described by the Landau-Zener theory.[4,5] It has also been established that nonadiabatic transitions between Rydberg states in a rapidly rising electric field can influence the threshold behavior exhibited in pulsed-field ionization.[6]

We present here an experimental study of the Landau-Zener effect carried out with Rydberg states of lithium in a strong electric field. In contrast to the case of molecular collisions, all the parameters can be controlled accurately, and the system comes close to the idealization of the basic Landau-Zener theory. Thus one has the opportunity to demonstrate quantitatively a basic dynamical process. The research is also motivated by the need to understand the experimental and theoretical systematics which govern field ionization in many applications. In the following sections we will discuss in turn the elementary Landau-Zener theory, corrections to the theory, the energy level structure of the test system (lithium), the experimental details, and our results.

II. THEORY OF NONADIABATIC TRANSITIONS AT AN AVOIDED CROSSING

A. The Landau-Zener effect

Before discussing dynamical behavior at an avoided crossing in detail, it is helpful to recapitulate the important features of the theory. We are concerned with a system whose Hamiltonian depends on some variable parameter q, such as the internuclear separation between two atoms or the amplitude of an applied electric or magnetic field. Of particular interest are two eigenstates of the system whose energy levels, to first approximation, cross for some value of q, as in Fig. 1(a).

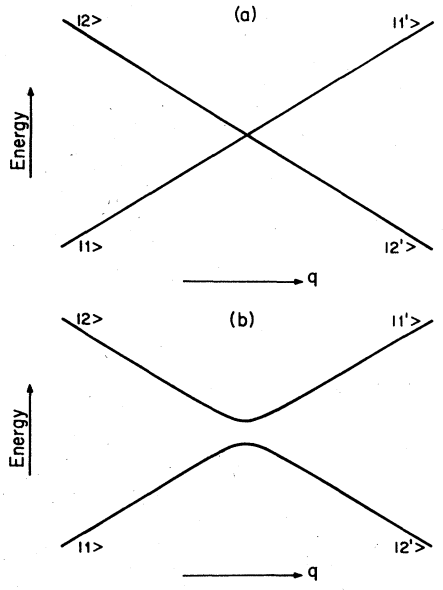

FIG. 1. Energy of the two-level system as a function of the parameter q. (a) Unperturbed energies. (b) An avoided crossing.

If the Hamiltonian is perturbed by an interaction $\mathcal{V}$ which couples the levels, the degeneracy at the crossing is broken. The levels repel, as in Fig. 1(b), in accordance with the "no-crossing" theorem.[7]

Consider a system initially prepared in state $|2\rangle$ of Fig. 1(b). If q then increases in time, sweeping the energies through the avoided crossing, will the system emerge in state $|2'\rangle$, or in state $|1'\rangle$? For the simplest case, where the unperturbed energy separation $E = E_1 - E_2$ varies linearly with q, as in Fig. 1(a), and q changes linearly with time, then the probability that the system will undergo a transition to $|2'\rangle$ is

$$P = \exp\left(-2\pi \frac{|\mathcal{V}_{12}|^2}{\hbar(dE/dt)}\right). \tag{1}$$

Here $\mathcal{V}_{12}$ is the matrix element of $\mathcal{V}$ connecting the two states, and $dE/dt = (dE/dq)(dq/dt)$ is the slew rate. It is evident that the behavior at the avoided crossing depends on the slope of the energy levels and the rate at which q changes compared to $|\mathcal{V}_{12}|$. In the limit $\mathcal{V}_{12} \to 0$, $P \to 1$, and the crossing is said to be traversed diabatically. In the opposite limit where $|\mathcal{V}_{12}|^2/\hbar$ is very large compared to the slew rate $P \to 0$ and the avoided crossing is said to be traversed adiabatically. Of more general interest is the intermediate case in which the behavior is neither purely adiabatic nor purely diabatic.

B. Dynamical equations

We consider a two-level system governed by a Hamiltonian $\hbar H_0(q)$ which depends explicitly on a parameter q. Denoting the eigenfunctions of $\hbar H_0$ by $|1\rangle$, $|2\rangle$, and expressing energies in frequency units, we have

$$H_0(q)\,|1\rangle = \Omega_1(q)\,|1\rangle, \tag{2a}$$

$$H_0(q)\,|2\rangle = \Omega_2(q)\,|2\rangle, \tag{2b}$$

where $\Omega_{1,2}(q)$ are the eigenenergies. We assume that the eigenvectors $|1\rangle$, $|2\rangle$ do not vary with q, and that $H_0(q)$ possesses a symmetry which permits degeneracy of the energy levels at some value of q. In the vicinity of the crossing, the energy levels are taken to vary linearly with q, as shown by the dashed lines in Fig. 2.

Next we consider the effect of a perturbation V which lacks the symmetry of H_0 and breaks the degeneracy at the crossing. The total Hamiltonian is

$$\hbar H = \hbar H_0 + \hbar V. \tag{3}$$

The matrix of H in the ordered basis $\{|1\rangle, |2\rangle\}$ is

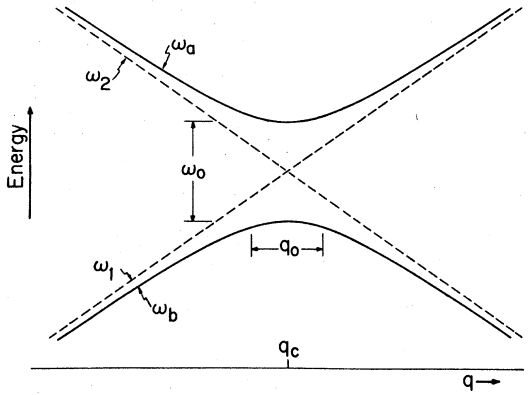

FIG. 2. Energy of the two-level system as a function of the parameter q. The dashed lines are the diagonal energies of H, and the solid lines are its eigenergies.

$$H(q) = \begin{pmatrix} \omega_1(q) & \frac{1}{2}\omega_0 e^{-i\phi} \\ \frac{1}{2}\omega_0 e^{i\phi} & \omega_2(q) \end{pmatrix}, \tag{4}$$

where

$$\omega_1(q) = \Omega_1(q) + \langle 1 \,|\, V \,|1\rangle, \tag{5a}$$

$$\omega_2(q) = \Omega_2(q) + \langle 2 \,|\, V \,|2\rangle, \tag{5b}$$

$$\tfrac{1}{2}\omega_0 = |\langle 1 \,|\, V \,|2\rangle|, \tag{5c}$$

$$\langle 1 \,|\, V \,|2\rangle = \tfrac{1}{2}\omega_0 e^{-i\phi}, \quad 0 \le \phi < 2\pi. \tag{5d}$$

We assume that V is independent of q so that ω_0 is a constant. The diagonal matrix elements of V shift the location of the crossing but do not affect the dynamics of the system.

The eigenenergies of H are

$$\omega_a(q) = \tfrac{1}{2}\{(\omega_1 + \omega_2) + [\omega(q)^2 + \omega_0^2]^{1/2}\}, \tag{6a}$$

$$\omega_b(q) = \tfrac{1}{2}\{(\omega_1 + \omega_2) - [\omega(q)^2 + \omega_0^2]^{1/2}\}, \tag{6b}$$

where $\omega(q) = \omega_1 - \omega_2$. The "crossing value" of the parameter, q_c, is defined by $\omega(q_c) = 0$. The energies (in frequency units) are shown by the solid lines in Fig. 2. The avoided crossing can be characterized by its separation, ω_0, and its width q_0 defined by

$$q_0 = \omega_0 \Big/ \left(\frac{d\omega}{dq}\right)_{q_c}. \tag{7}$$

The eigenfunctions of H are conveniently written in terms of the phase angle ϕ [Eq. 5(d)] and the parameter θ defined by

$$\tan\theta(q) = \frac{\omega_0}{\omega(q)}, \quad 0 \le \theta < \pi. \tag{8}$$

A set of orthonormal eigenvectors is

$$|a(q)\rangle = \cos\left(\frac{\theta(q)}{2}\right) e^{-i\phi/2}|1\rangle + \sin\left(\frac{\theta(q)}{2}\right) e^{i\phi/2}|2\rangle, \tag{9a}$$

$$|b(q)\rangle = -\sin\left(\frac{\theta(q)}{2}\right) e^{-i\phi/2}|1\rangle + \cos\left(\frac{\theta(q)}{2}\right) e^{i\phi/2}|2\rangle. \tag{9b}$$

$|a(q)\rangle$ and $|b(q)\rangle$ have energies ω_a and ω_b, respectively.

Now let us examine the effect of time variations in q. The time-dependent Schrödinger equation

$$H|\Psi(t)\rangle = i\frac{\partial|\Psi(t)\rangle}{\partial t} \tag{10}$$

may be solved by taking

$$|\Psi(t)\rangle = C_1(t)\exp\left(-i\int_0^t \omega_1 dt'\right)|1\rangle + C_2(t)\exp\left(-i\int_0^t \omega_2 dt'\right)|2\rangle. \tag{11}$$

Substituting Eq. (11) into (10) and using (5) results in

$$i\dot{C}_1 = \tfrac{1}{2}\omega_0 e^{-i\phi}\exp\left(i\int_0^t \omega\, dt'\right)C_2, \tag{12a}$$

$$i\dot{C}_2 = \tfrac{1}{2}\omega_0 e^{i\phi}\exp\left(-i\int_0^t \omega\, dt'\right)C_1. \tag{12b}$$

These may be decoupled to yield

$$\ddot{C}_1 - i\omega(t)\dot{C}_1 + \frac{\omega_0^2}{4}C_1 = 0, \tag{13a}$$

$$\ddot{C}_2 + i\omega(t)\dot{C}_2 + \frac{\omega_0^2}{4}C_2 = 0. \tag{13b}$$

For a particular initial state, initial values of C_1 and C_2 are determined by Eqs. (8), (9), and (11), and values of $\dot{C}_1$ and $\dot{C}_2$ are given by Eqs. (12).

We are concerned with the behavior of the system over an interval starting at time t_i and ending at time t_f, during which the parameter q changes from q_i to q_f. Assume that the initial state is $|b_i\rangle$, where $b_i = b(q_i)$. The probability that the final state is $|a_f\rangle$, i.e., that the system has "jumped" or made a diabatic transition from $|b\rangle$ to $|a\rangle$, is

$$P = |\langle\Psi(t_f)|a_f\rangle|^2. \tag{14}$$

If q varies linearly in time, so that $d\omega/dt$ is constant, then Eqs. (13) can be solved.[2] The probability is most conveniently expressed in terms of the parameter

$$\Gamma = \frac{\omega_0^2}{4\left(\frac{d\omega}{dt}\right)} = \frac{|\langle 1|V|2\rangle|^2}{\frac{d\omega}{dt}}, \tag{15}$$

where the derivative is evaluated at the crossing. In the limit $t_i \to -\infty$, $t_f \to +\infty$, the result is given by Eq. (1):

$$P = e^{-2\pi\Gamma}.$$

C. Corrections to the Landau-Lener formula

The conditions assumed for the Landau-Zener theory are never fully satisfied in practice. In order to investigate corrections to the Landau-Zener formula, we have obtained solutions to Eqs. (13) by numerical integration. This permits us to impose arbitrary initial conditions, and to allow $q(t)$ to vary as pleased. Although the corrections required by our particular experimental system will turn out to be negligible, some insight can be gained by investigating their nature. Equations (13) can be integrated by making the substitutions

$$C_1 = U_1\exp\left(\frac{i}{2}\int_0^t \omega\, dt'\right), \tag{16a}$$

$$C_2 = U_2\exp\left(-\frac{i}{2}\int_0^t \omega\, dt'\right). \tag{16b}$$

After some rearrangement, we obtain

$$\ddot{U}_1 + \tfrac{1}{4}(\omega_0^2 + 2i\dot{\omega} + \omega^2)U_1 = 0, \tag{17a}$$

$$\ddot{U}_2 + \tfrac{1}{4}(\omega_0^2 - 2i\dot{\omega} + \omega^2)U_2 = 0, \tag{17b}$$

which can be integrated by a modified Numerov method, as described in the Appendix.

In our experiments, the relative slope of the energy levels $d\omega/dq$ is very nearly constant. The time dependence of q, however, differs significantly from the assumed linear variation over all time. In practice, q sweeps through the avoided crossing linearly, but is effectively constant outside of some time interval τ. Figure 3(a) shows how q and the energies vary in the Landau-Zener case. Figure 3(b) shows their variations for an idealized fast pulse situation, and Fig. 3(c) shows their variations for a more realistic fast pulse.

A good approximation to the behavior of ω is

$$\omega(t) = \alpha\tau\left(\frac{1}{[1+\exp(-4t/\tau)]} - \frac{1}{2}\right) \tag{18}$$

which has the properties

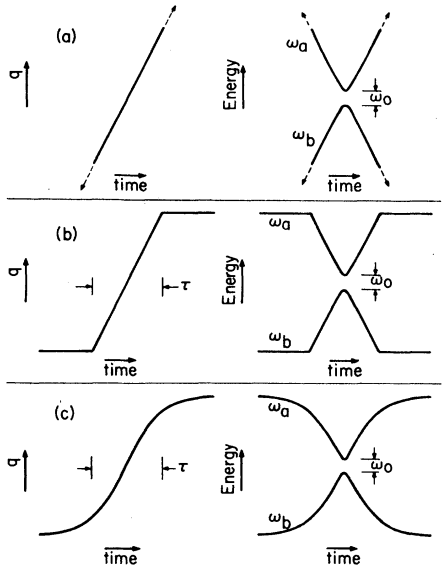

FIG. 3. Possible time variations of q and the corresponding eigenenergies. (a) $q(t)$ linear and extends over all time; the Landau-Zener case. (b) $q(t)$ linear over a finite range; an idealized "fast pulse". (c) $q(t)$ for a more realistic fast pulse; the corresponding $\omega(t)$ is given by Eq. (18).

$$\omega(t)=\begin{cases}\frac{-1}{2}\alpha\tau, & t\to-\infty\\ \alpha t, & |t|\ll\tau\\ \frac{+1}{2}\alpha\tau, & t\to\infty.\end{cases} \tag{19}$$

Note that the slew rate through the avoided crossing $d\omega/dt=\alpha$ is independent of the length of the sweep τ. The transition probability now depends on the parameter $\Gamma=\omega_0^2/(4\alpha)$, which characterizes "how adiabatically" the avoided crossing is traversed, and a second parameter

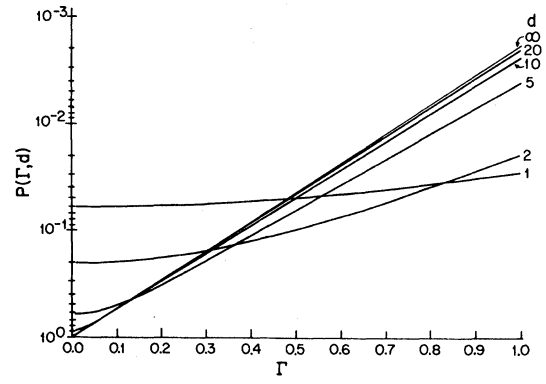

FIG. 4. Diabatic transition probability P as a function of Γ for various values of d. The thin line is the Landau-Zener result ($d=\infty$).

$$s=\frac{\omega_0\tau}{2}, \tag{20}$$

which is essentially the ratio of the level separation to the spectral width of the parameter q. A third related parameter is

$$d=\frac{s}{\Gamma}=\frac{2\alpha\tau}{\omega_0} \tag{21}$$

which is twice the ratio of the total change in energy during the sweep to the separation at the avoided crossing. For $d\to\infty$, we have the Landau-Zener case. In general, we can write the transition probability as $P(\Gamma,d)$, with

$$P(\Gamma,\infty)=e^{-2\pi\Gamma}. \tag{22}$$

Values of $P(\Gamma,d)$ obtained by numerical integration are displayed in Fig. 4. For $d\gtrsim 20$, the diabatic transition probability generally agrees with the Landau-Zener result. It is interesting to note that for $s\sim 1$, $P(\Gamma,s)$ displays a quasiresonant behavior, as shown in Fig. 5. The maximum can exceed the Landau-Zener value by 0.05, which in some cases represents a factor of 2 enhancement.

D. Resonance transitions at an avoided crossing

Experimental verification of the dynamics of traversing an avoided crossing requires, among other things, determining the level separation ω_0. Resonance spectroscopy of the level structure is by far the most accurate way to accomplish this, assuming that the parameter q is an applied electric or magnetic field. In this section we discuss the systematics of resonance: the behavior of an

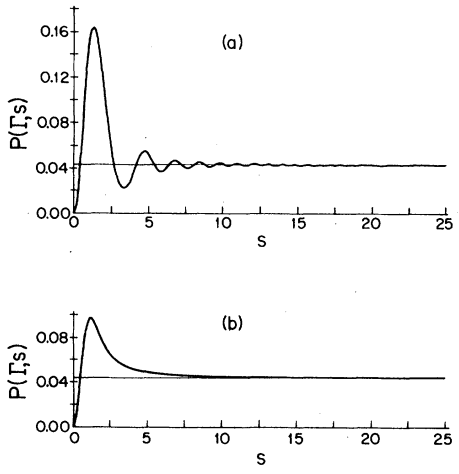

FIG. 5. Diabatic transition probability as a function of s for $\Gamma=0.5$. The thin lines are the Landau-Zener prediction. (a) $q(t)$ given by Fig. 3(b); the "sharp corners" in $q(t)$ produce oscillations. (b) $q(t)$ given by Fig. 3(c).

avoided crossing system under a periodic perturbation.

We wish to predict the response of the system to a sinusoidally varying field $q(t)$ centered on the crossing value q_c:

$$q(t) = q_c + q_r \cos\omega_r t . \tag{23}$$

In the vicinity of the avoided crossing, the Hamiltonian can be written

$$H = H(q_c) + (q - q_c) V' . \tag{24}$$

It is convenient to represent the matrix of H in a basis which diagonalizes $H(q_c)$. From Eqs. (6) and (9) we have

$$\omega_A = \omega_b(q_c) , \quad \omega_B = \omega_b(q_c) , \tag{25a}$$

$$|A\rangle = |a(q_c)\rangle , \quad |B\rangle = |b(q_c)\rangle . \tag{25b}$$

The matrix elements of V' are determined from the asymptotic slopes of the avoided crossing.[8] The Hamiltonian represented in the ordered basis $\{|A\rangle, |B\rangle\}$ is

$$H = \begin{pmatrix} \omega_A + L\cos\omega_r t & M\cos\omega_r t \\ M\cos\omega_r t & \omega_B + L\cos\omega_r t \end{pmatrix} , \tag{26}$$

where

$$L = \tfrac{1}{2} q_r (\partial/\partial q)(\omega_1 + \omega_2)\,|_{q_c} , \tag{27a}$$

$$M = -\tfrac{1}{2} q_r (\partial/\partial q)(\omega_1 - \omega_2)\,|_{q_c} . \tag{27b}$$

For the case of a symmetric avoided crossing, say as in Fig. 2, then $L = 0$, and the problem reduces to resonance in a standard two-level system. With the condition of small amplitude $|q_r| \ll |q_0|$, the eigenstates of H are essentially $|A\rangle$ and $|B\rangle$, and the Rabi formula follows.

Resonance at an avoided crossing exhibits two pecularities which must be borne in mind. The first is that the oscillating matrix elements can easily be so large that the rotating-wave approximation breaks down. The second is that the states $|a(q)\rangle$ and $|b(q)\rangle$ themselves vary if the field is swept, so that there is a real physical difference between sweeping the field and sweeping the frequency. Analysis of the behavior for fields not centered on the avoided crossing, omitted here, is straightforward.

The numerical methods described in the last section are quite general and can also be applied to the case of an oscillating field $q(t)$ of any amplitude. We have confirmed that at low-field amplitudes the transition probability obeys the Rabi formula as expected.

III. AVOIDED CROSSINGS IN STARK STATES OF OF LITHIUM

Stark states of highly excited (Rydberg) atoms display a multitude of avoided crossings, many of which provide excellent test systems for observing the Landau-Zener effect. The Stark structure of Rydberg alkali-metal atoms has been analyzed by Zimmerman *et al.*[9]; we summarize here some of the relevant results.

The Stark structure of hydrogen can serve as the starting point for understanding the Stark structure of alkali-metal Rydberg atoms. The electronic Hamiltonian, neglecting spin and relativistic effects, is

$$H_0 = -\tfrac{1}{2}\nabla^2 - 1/r + Fz , \tag{28}$$

where the applied field is $F\hat{z}$ and atomic units are used ($\hbar = m = e = 1$). Angular momentum along the z axis commutes with H_0 and is a constant of motion. There is a second constant of motion, a generalized Lenz-Pauli vector,[10] which also commutes with H_0. The existence of this constant of motion has several consequences: The problem is separable, the states display a first-order Stark effect (i.e., they possess permanent dipole moments), and degeneracies between levels are allowed, even for the same value of m. When considering a map of the energy levels, this last property permits the Stark levels of hydrogen to cross.

The eigenvalues of H_0 are

$$E(n, n_1, n_2, m) = -\frac{1}{2n^2} + \tfrac{3}{2} n(n_1 - n_2)F + O(F^2) , \tag{29}$$

where n is the principal quantum number and n_1 and n_2 are the parabolic quantum numbers which satisfy $n_1 + n_2 + |m| + 1 = n$. The higher-order terms, which arise from mixing between principal manifolds, do not affect the symmetry of the problem. These contributions alter the eigenfunctions, but their effect is small and we can treat the eigenfunctions as constant in the limited field range of interest near a specific crossing.

The generalized Lenz-Pauli vector is a constant of motion only if the central potential varies exactly as $-1/r$. If the Coulomb potential is slightly perturbed this dynamical symmetry is lost, the problem is no longer separable, and the sharp crossings are converted to avoided crossings. If the perturbation is small, however, the size of the avoided crossings is small, vanishing as the perturbation approaches zero.

A natural way to characterize short-range perturbations to the Coulomb potential is by introducing a quantum defect δ_l into the eigenenergy of a particular zero-field angular momentum state,

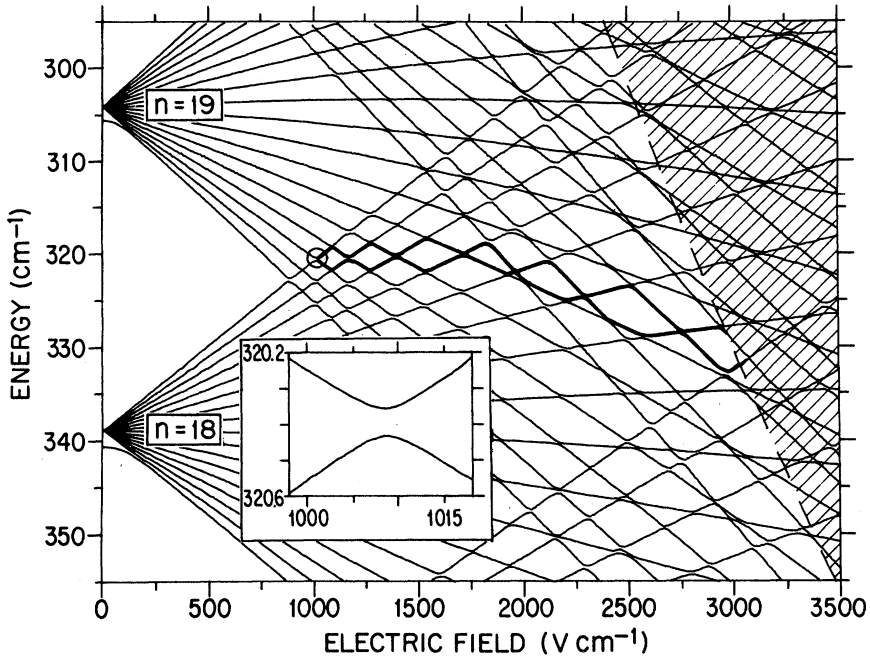

FIG. 6. Stark energies of lithium $|m|=1$ vs electric field. The avoided crossing observed is encircled and shown in detail by the inset. The dashed line is the classical ionization limit (Ref. 15). The heavy lines show the adiabatic paths followed by the two states. Avoided crossing sizes are exaggerated by the plotting routine.

whose energy becomes $E(n,l) = -1/[2(n-\delta_l)^2]$. Physically, the quantum defect represents a phase shift introduced into the wave function by the perturbation. The perturbation destroys the dynamical symmetry and the level crossings are converted to avoided crossings. We should expect that for a single quantum defect δ, the size of the avoided crossings vanishes as $\delta \to 0$. Komarov, Grozdanov, and Janev[11] have shown that this is indeed the case.

For experimental reasons which will be discussed in the next section, the avoided crossing chosen for study occurs between $n=18$ and 19, and $|m|=1$ levels of lithium. Figure 6 shows the avoided crossing and the calculated Stark structure in its vicinity. These were calculated following the procedures of Zimmerman *et al.*[9]

IV. EXPERIMENT

In this section we describe the experimental design, the apparatus, and the method in which each variable entering the Landau-Zener theory is determined.

A. Experimental design

The states comprising the avoided crossing, shown circled in Fig. 6, are $|2\rangle = (19,2,15,1)$ and $|1\rangle = (18,16,0,1)$ where $(n, n_1, n_2, |m|)$ denotes a set of parabolic quantum numbers. The experiment works as follows: Either of the two states $|a_i\rangle$ or $|b_i\rangle$ is populated by pulsed laser excitation at a field F_i slightly below F_c. The field is then swept through the avoided crossing with a fast but known slew rate to a final value $F_f > F_c$. The transition probability is determined by measuring the populations of the final states $|a_f\rangle$ and $|b_f\rangle$. This is accomplished by applying a relatively slowly increasing field to carry $|a_f\rangle$ and $|b_f\rangle$ to their field-ionization thresholds along the paths indicated in Fig. 6.

A number of reasons dictated the choice of lithium and the selection of the particular avoided crossing. The lithium Rydberg states are conveniently reached with our lasers, and the Stark structure is sufficiently large for the levels to be resolved. The avoided crossings of the $|m|=1$ states are small enough to yield significant transition probabilities with the slew rates which we could achieve. The reason for choosing this particular crossing from the multitude of candidates is that its states ionize at fields which differ by about 70 V cm^{-1}, allowing them to be completely resolved by field-ionization methods.

B. Apparatus

A schematic diagram of the experimental arrangement is shown in Fig. 7. An atomic beam of lithium provided a density of 10^9 atoms cm^{-3} in

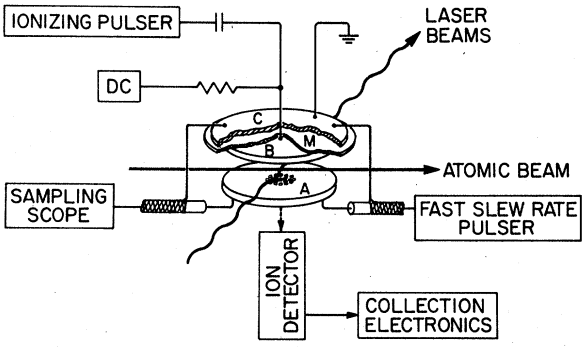

FIG. 7. Schematic diagram of the experimental system. A and B are field plates, C is a ground plane, and M is an insulating Mylar film.

the interaction region with a mean speed of 1.6 mm μsec^{-1}. The atoms were excited by pulsed tunable dye-laser light directed perpendicularly to the atomic beam. A three-step excitation scheme was used: $2s \rightarrow 2p$ (671 nm), $2p \rightarrow 3s$ (813 nm), and finally $3s \rightarrow$ Rydberg state (626 nm). The polarization of the final laser was perpendicular to the electric field so that only $|m| = 1$ states were excited.

The pulses from the first two dye lasers were simultaneous, but the final pulse was delayed until the initial pulses were extinguished. The dye lasers were of the "grazing-incidence" type[12]; the initial two lasers had a linewidth of about 0.4 cm^{-1} and the final laser, which used a double grating configuration, had a linewidth of about 0.1 cm^{-1}. The dye lasers were pumped by harmonics of a Quanta-Ray DCRIa Nd:YAG laser and produced peak powers of a few kilowatts.

The excitation region was centered between two parallel electric-field plates which were separated by 4.95(3) mm. The Rydberg states were prepared in a dc field, F_i, about 15–20 V cm^{-1} below the crossing field $F_c = 1008(1)$ V cm^{-1}. This field was supplied by a well regulated high-voltage source connected to the upper-field plate.

The excited atomic states were swept through the avoided crossing with a fast voltage pulse starting 100 nsec after excitation. The populations of the final states were analyzed by selective field ionization. The ions were accelerated by the field and passed through the lower plate via a number of small holes to an electron multiplier.

C. Pulsed electric field

A two-step pulsed field was generated with two independent supplies. The first step, the "fast slew" pulse, carried the system through the avoided crossing with an accurately controlled slew rate which could be varied between 7 and 40 kV cm^{-1} μsec^{-1}. In order to prevent traversing a second avoided crossing, the amplitude of the fast slew pulse was limited to 40 V cm^{-1}. The second step, the ionizing pulse, increased the field to 3 kV cm^{-1} in a time of 3 μsec. This pulse carried the system across the field-ionization threshold. About 100 V cm^{-1} below the threshold its slew rate decreased to approximately 50 V cm^{-1} μsec^{-1}. The fast slew pulse was generated with an avalanch transistor pulser.[13] The signal was coupled out through a Hewlett-Packard 355 CVHF variable attenuator which allowed the amplitude to be varied without altering the pulse shape.

The field-plate structure shown in Fig. 7 was adopted in order to provide continuous monitoring of the slew rate and to avoid reflections or unnecessary loading of the fast slew pulse. The pulse was applied to the lower plate A across a matched load connected to the ground plane C. The matched load was a 50 ohm transmission line leading to a sampling scope (Tektronix 7904, 7T11, and 7S11 sampling units, S6 head).

The ionizing pulse and dc bias voltage were coupled to the upper-field plate B. This plate was capacitively coupled to the ground plane through a thin Mylar sheet. The capacitance was large enough to transmit the fast slew pulse, but small enough to permit application of the much slower ionizing pulse.

Uncertainty in the slew rate was one of the limiting errors in our measurement, and jitter in the triggering of the sampling scope was a principal contributor to this error. Jitter was minimized by triggering the scope directly from the fast slew pulser. This required a 50 nsec delay line between the pulser and the field plates, which attenuated the signal and limited the rate. Over the range available with this method, however, the slew rate could be determined to 4%. To achieve the higher slew rates, the scope was triggered ahead of the fast slew pulser. The estimated uncertainty by this method is 10%. Data taken by both methods are identified in the final results (see Fig. 10).

D. Structure of the avoided crossing

The energy level slopes in lithium near the avoided crossing $d\omega/dF$ were calculated using the methods of Zimmerman *et al.*,[9] and were also measured by experimentally mapping the Stark structure. The result is $d\omega/dF = 3.47(1) \times 10^{-2}$ cm^{-1}/V cm^{-1}). The size of the avoided crossing is far more difficult to calculate than the energy level slopes, depending as it does on high numerical precision and accurate input data in the form of quantum defects. Using the quantum-defect data of Johansson,[14] we obtained $\omega_0 = 7.7(1) \times 10^{-2}$ cm^{-1}. Since this value was not sufficiently accu-

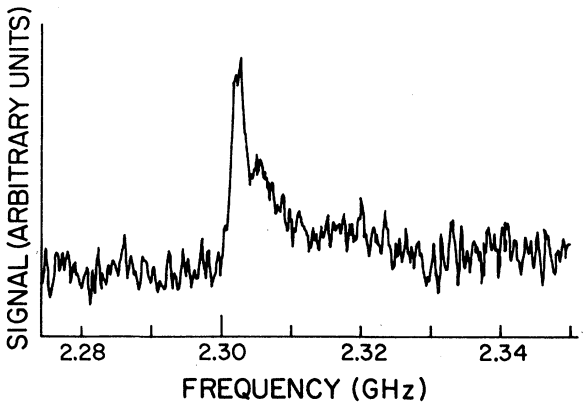

FIG. 8. Resonance curve for the avoided crossing; signal proportional to rf transition probability vs frequency.

rate for our purpose, we measured the separation directly by radio-frequency (rf) spectroscopy.

A single level was populated at the avoided crossing field $F_c = 1008$ V cm^{-1}. Although the pulsed dye laser was too broad to resolve the levels, the oscillator strength for the optical transition at the avoided crossing is concentrated in the lower level so that only the lower level was excited. Transitions to the upper level were induced by an rf voltage applied between the field plates. The resonance signal was monitored by measuring the relative population of the states. The oscillator strength for the rf transition is large, $f = 0.1$, and a power of $\sim 10^{-7}$ W was adequate. The power was supplied by a Hewlett-Packard 86290B signal generator, and the frequency was monitored by a counter.

Figure 8 shows a typical resonance signal. The asymmetry is due to field inhomogeneities and the quadratic dependence of the level separation on the field near the avoided crossing. In spite of the relatively poor line shape and signal-to-noise ratio, the avoided crossing separation was determined to an accuracy entirely adequate for our purpose. The result from seven independent measurements is $\omega_0 = 7.6820(12) \times 10^{-2}$ cm^{-1}.

E. Systematics pulsed-field ionization

Selective ionization with a pulsed field was used to analyze the populations of the two levels after the avoided crossing was traversed. This technique requires a one-to-one mapping between each energy level of a Rydberg atom at low and high electric field, and a unique threshold field for ionizating each level. A number of assumptions underlies the application of this method, and these warrant some discussion.

The threshold field for ionization is $F = W^2/4$, where W is the energy of the level in the field.[15] (The threshold region shown in Fig. 6 is given by this expression.) Although the concept of a threshold field has been widely accepted, it is important to recognize that it applies only to the energetics of ionization and provides no information about ionization rates. For atoms with an unperturbed Coulomb atomic potential, the ionization rate can be negligible at fields well in excess of the threshold field. In the case of low $|m|$ states of the alkali-metal atoms, however, the ionization rates are generally observed to become large, typically greater than 10^7 sec^{-1}, abruptly at the threshold. Nevertheless, in applications where the applied ionizing field increases rapidly in time, the effect of a finite (and nonmonatonic) ionization rate can significantly alter the observed signal. If the goal is only to monitor the occurrence of transitions between states, as in microwave resonance spectroscopy of Rydberg states, then any alteration of the ionization signal can be used as an indicator and effects due to finite ionization rates may not be important. If the need is to measure transition probabilities quantitatively, however, effects due to the field dependence of the ionization rates must be taken into account. One way to minimize these effects is to traverse the threshold region slowly by introducing a "break" into the ionization field slew rate, as described in Section IV C.

A second consideration in determining final-state populations is that their threshold fields must be well resolved. For adjacent levels there is no simple way to predict this. Inspection of Fig. 6, for instance, reveals that the levels are by no means uniformly spaced on the threshold curve. Determining whether any given pair of adjacent levels can be resolved requires either careful computation of the level structure, or an experimental survey of the region.

The fundamental question of pulsed-field ionization, however, is whether the initial state evolves adiabatically or diabatically to the high field region. For a hydrogenic atom the level crossings are so sharp that diabatic traversals are the rule; for low $|m|$ states of the alkali-metal atoms all crossings are avoided, and the repulsions are so strong that the traversals are almost invariably adiabatic. Unfortunately there is no simple rule of thumb for connecting high- and low-field states. Any particular case, however, can be analyzed by investigating the Stark structure of the system.

The energy level routes followed by the states of interest in this experiment are shown in Fig. 9, which is blown up from Fig. 6. The size of the avoided crossings can be reliably estimated from the drawing, and it is apparent that during the ionization process the levels undergo a large

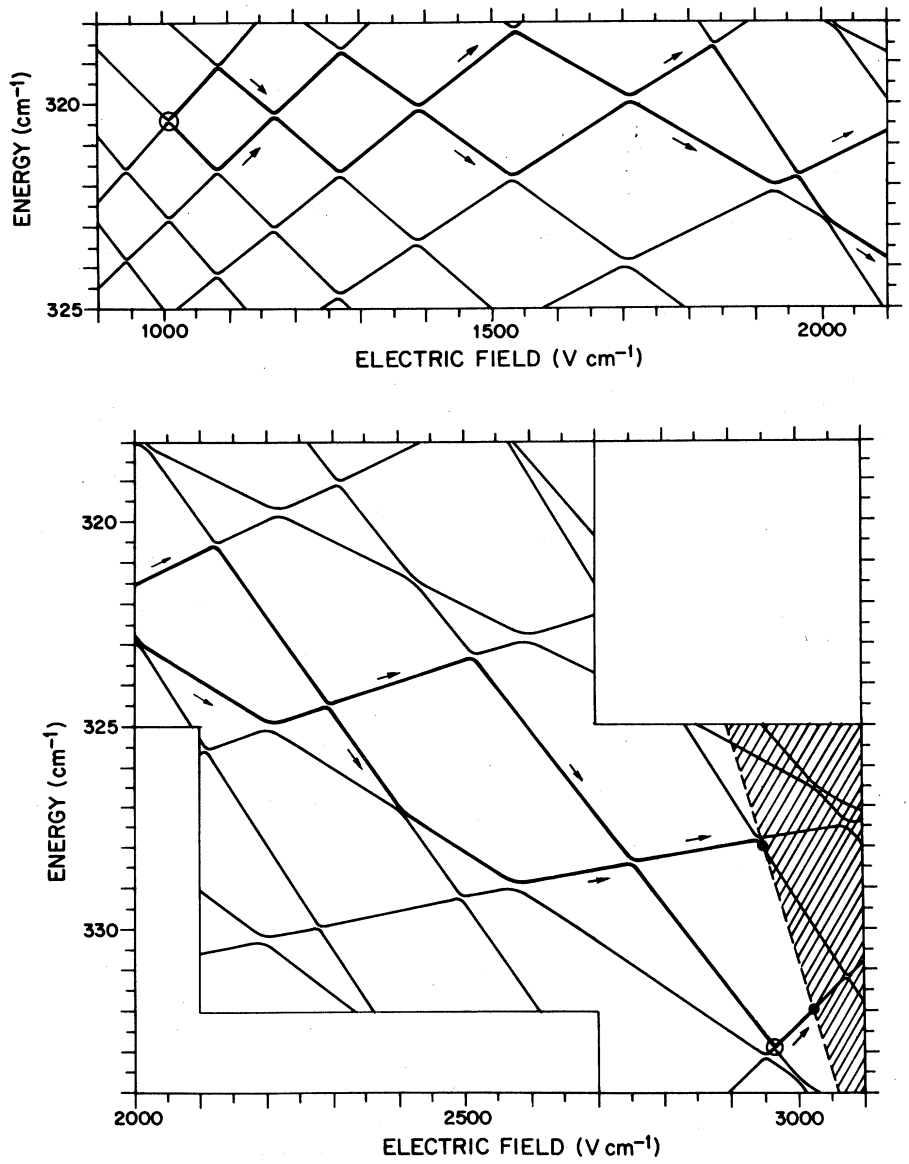

FIG. 9. Details from Fig. 6 of the adiabatic paths followed by the states during pulsed ionization. The avoided crossing sizes are authentic. The circled feature near the ionization limit is discussed in the text.

series of avoided crossings comparable in magnitude to the one under study. A typical avoided crossing in this region has a separation of 0.07 cm^{-1}. The Landau-Zener parameter for the transition is calculated to be $\Gamma = 1.7$ and yields a transition probability $P \sim 10^{-5}$. This indicates that branching to unwanted levels is not likely to be a serious problem.

An unusual feature occurs very close to the threshold: a weakly avoided crossing shown circled in Fig. 9. Although this crossing does not cause any branching in our experiment, it is important to realize that "sharp" crossings such as this can occur sporadically and can lead to a branching of paths in the threshold.

F. Determining the diabatic transition probability

The final-state populations, n_a and n_b, were measured with two gated integrators that were triggered from the ionizing voltage so that the gates were centered about the threshold field for each state. The signals were digitized and the transition probability $P = n_a/(n_a + n_b)$ was evaluated at each cycle of operation. This procedure reduced much of the effect of fluctuations in the laser intensity.

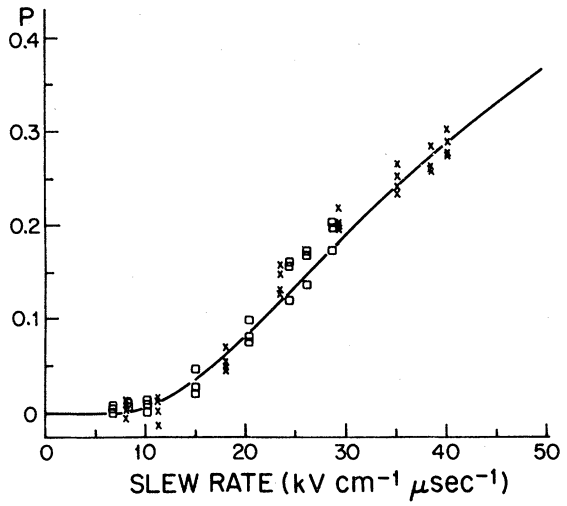

FIG. 10. Diabatic transition probability P as a function of the fast pulser slew rate. Data taken with and without the delay line discussed in Sec. IV C are shown by □ and X, respectively. The solid line is calculated with no adjustable parameters.

The major source of systematic error was unequal ion detector efficiency for the two states due to the effects of motion in the atomic beam across the positions of the grid holes in the lower plate through which the ions pass to the multiplier. This error was minimized by moving the excitation region to a position which yielded the same transition probability irrespective of which initial state was populated.

A small transfer between the two states (~3%) occurred because of extraneous effects such as blackbody radiation and collisions. In addition, there were small electronic offsets between the two channels. These effects were monitored by periodically carrying out the measurement without applying the fast slew pulse, and also by setting the bias field slightly above the avoided crossing. The measured diabatic probability was then corrected for these errors. With these procedures, systematic errors in measuring the transition probability are believed to be small compared to the statistical error, typically 0.03.

V. RESULTS AND DISCUSSION

Under our experimental conditions, the parameter d [Eq. (21)] ranged between 28 and 38. According to the discussion in Sec. II C, the diabatic transition probability under these conditions is given with great accuracy by the simple Landau-Zener expression, Eq. (1). With the range of slew rates we could achieve, 7–40 kV cm^{-1} μsec^{-1}, Γ varied between 1.1 and 0.2, and the calculated diabatic transition probability varied between 7×10^{-4} and 0.28. Although it would have been desirable to investigate conditions of higher transition probabilities, the demands on the slew rate were prohibitive. For instance, achieving a probability of 0.5 would require a slew rate greater than 70 kV cm^{-1} μsec^{-1}.

The experimental results are presented in Fig. 10. The scatter is due to jitter in the slew rate, discussed in Sec. IV C, and statistical fluctuations in the measurement of the transition probability. We believe that the limits of possible systematic errors are small compared to the statistical errors, and that the experimental results are in good agreement with theory.

In addition to demonstrating the Landau-Zener effect, this work was motivated by the need to understand the dynamics of Rydberg atoms in rapidly rising electric fields. We believe that this goal has been substantially achieved, and that the insights it provides should be considered in planning applications of pulsed-field ionization.

ACKNOWLEDGMENTS

We thank W. Mark Finlay, Mark D. Havey, and William D. Phillips for contributions to the preliminary work on this project. We also thank Jarbas C. Castro, A. Ganesh Vaidyanathan, William P. Spencer, Myron L. Zimmerman, and Frank Laloë for helpful discussions. This work was supported by the Department of Energy under Contract No. EG775 024 370; one of us (M.M.K.) was the recipient of an NSF graduate fellowship.

APPENDIX: NUMEROV ALGORITHM FOR A COMPLEX DIFFERENTIAL EQUATION

Equations (17) are second-order, linear, complex differential equations with no first-order term. The general form is

$$C''=w(t)C\,.$$

It is convenient to consider the real and imaginary parts of this equation

$$a''=g(t)a-j(t)b\,,$$

$$b''=g(t)b+j(t)a\,,$$

where $a = \mathrm{Re}\,C$, $b = \mathrm{Im}\,C$, $g(t) = \mathrm{Re}\,w(t)$, and $j(t) = \mathrm{Im}\,w(t)$. Proceeding as in the standard Numerov method, we obtain the "stepping" equations

$$a_{i+1} = \frac{1}{\beta_{i+1}}\left(1 + \frac{j_{i+1}^2}{\beta_{i+1}^2}h^4\right)^{-1}\left[-\left(\beta_{i-1} + \frac{j_{i-1}j_{i+1}}{\beta_{i+1}}h^4\right)a_{i-1} + \left(\alpha_i - \frac{10 j_i j_{i+1}}{\beta_{i+1}}h^4\right)a_i \right.$$
$$\left. + h^2\left(j_{i+1}\frac{\beta_{i-1}}{\beta_{i+1}} - j_{i-1}\right)b_{i-1} - h^2\left(10 j_i + j_{i+1}\frac{\alpha_i}{\beta_{i+1}}\right)b_i\right] + O(h^6)\,,$$

$$b_{i+1} = \frac{1}{\beta_{i+1}}\left[-\beta_{i-1}b_{i-1} + \alpha_i b_i + h^2(j_{i-1}a_{i-1} + 10 j_i a_i + j_{i+1}a_{i+1})\right] + O(h^6)\,,$$

where $\alpha_i = 24 + 10 g_i h^2$, $\beta_i = 12 - g_i h^2$. Initiating the integration requires values for a_1 and b_1. These can be obtained from a_0, a_0', b_0, b_0', and by using a Taylor series expansion

$$a_1 = (1 + \tfrac{1}{2} g_0 h^2)a_0 + a_0' h - \tfrac{1}{2} j_0 b_0 h^2 + O(h^3)\,,$$
$$b_1 = (1 + \tfrac{1}{2} g_0 h^2)b_0 + b_0' h + \tfrac{1}{2} j_0 a_0 h^2 + O(h^3)\,.$$

---

*Present address: Dept. of Mech. and Aeron. Engineering, Princeton University, Princeton, New Jersey 08540.

[1]L. D. Landau, Phys. Z. Sowjetunion 2, 46 (1932); L. D. Landau and E. M. Lifshitz, *Quantum Mechanics: Non-relativistic Theory*, 3rd ed. (Pergamon, New York, 1977), pp. 342–351.

[2]C. Zener, Proc. R. Soc. London Ser. A137, 696 (1932).

[3]T. F. O'Malley, *Advances in Atomic and Molecular Physics*, edited by D. R. Bates and I. Esterman (Academic, New York, 1971), Vol. 7, p. 223; W. Lichten, Phys. Rev. A 3, 594 (1971), and references therein.

[4]Adiabatic rapid passage can be visualized in a rotating coordinate system. The effective field is $[(B_0 - \omega/\gamma)^2 + B_1^2]^{1/2}$ where B_0 is the applied field and B_1 is a transverse field rotating at frequence ω. γ is the gyromagnetic ratio. The energies are $\pm\gamma B_{\mathrm{eff}}/2$. As B_0 or ω is varied, the system traverses the avoided crossing when when $\omega = \gamma B_0$.

[5]R. D. Hight, R. T. Robiscoe, and W. R. Thorson, Phys. Rev. A 15, 1079 (1977); T. A. Vartanyan, S. G. Prizbel'skii, and N. A. Chigir, Zh. Eksp. Teor. Fiz. 75, 439 (1978) [Sov. Phys.—JETP 48, 220 (1978)].

[6]T. F. Gallagher, L. M. Humphrey, R. M. Hill, and S. A. Edelstein, Phys. Rev. Lett. 37, 1465 (1976); T. H. Jeys, G. W. Foltz, K. A. Smith, E. J. Beiting, F. G. Kellert, F. B. Dunning, and R. F. Stebbings, *ibid.* 44, 390 (1980).

[7]E. Merzbacher, *Quantum Mechanics*, 2nd ed. (Wiley, New York, 1970), pp. 428–429.

[8]One uses parametric differentiation, otherwise known as the Feynman-Hellman theorem. Compare C. Cohen-Tannoudji, B. Diu, and F. Laloë, *Quantum Mechanics* (Wiley, New York, 1977), pp. 1192–1193.

[9]M. L. Zimmerman, M. G. Littman, M. M. Kash, and D. Kleppner, Phys. Rev. A 20, 2251 (1979).

[10]K. Helfrich, Theor. Chim. Acta 24, 271 (1972).

[11]I. V. Komarov, T. P. Grozdanov, and R. K. Janev, J. Phys. B 13, L573 (1980).

[12]M. G. Littman and H. J. Metcalf, Appl. Opt. 17, 2224 (1978); I. Shoshan, N. Danon, and U. Oppenheim, J. Appl. Phys. 48, 4495 (1977); M. G. Littman, Opt. Lett. 3, 138 (1978); I. Shoshan and U. Oppenheim, Opt. Commun. 25, 375 (1978).

[13]J. M. Ley, T. M. Christman, and C. G. Wildey, Proc. IEEE 117, 1057 (1970), Sec. 3.4.

[14]I. Johansson, Ark. Fys. 15, 169 (1959).

[15]M. G. Littman, M. M. Kash, and D. Kleppner, Phys. Rev. Lett. 41, 103 (1978). We have made the small corrections to the threshold field described in this reference.